JB Journals.ASM.org

Interaction Network and Localization of *Brucella abortus* Membrane Proteins Involved in the Synthesis, Transport, and Succinylation of Cyclic β-1,2-Glucans

Leticia S. Guidolin,[a] Susana M. Morrone Seijo,[a] Francisco F. Guaimas,[a] Diego J. Comerci,[a,b] Andrés E. Ciocchini[a]

Instituto de Investigaciones Biotecnológicas Dr. Rodolfo A. Ugalde, Instituto Tecnológico de Chascomús, Universidad Nacional de San Martín, CONICET, San Martín, Buenos Aires, Argentina[a]; Comisión Nacional de Energía Atómica, Grupo Pecuario, Centro Atómico Ezeiza, Buenos Aires, Argentina[b]

ABSTRACT

Cyclic β-1,2-glucans (CβG) are periplasmic homopolysaccharides that play an important role in the virulence and interaction of *Brucella* with the host. Once synthesized in the cytoplasm by the CβG synthase (Cgs), CβG are transported to the periplasm by the CβG transporter (Cgt) and succinylated by the CβG modifier enzyme (Cgm). Here, we used a bacterial two-hybrid system and coimmunoprecipitation techniques to study the interaction network between these three integral inner membrane proteins. Our results indicate that Cgs, Cgt, and Cgm can form both homotypic and heterotypic interactions. Analyses carried out with Cgs mutants revealed that the N-terminal region of the protein (Cgs region 1 to 418) is required to sustain the interactions with Cgt and Cgm as well as with itself. We demonstrated by single-cell fluorescence analysis that in *Brucella*, Cgs and Cgt are focally distributed in the membrane, particularly at the cell poles, whereas Cgm is mostly distributed throughout the membrane with a slight accumulation at the poles colocalizing with the other partners. In summary, our results demonstrate that Cgs, Cgt, and Cgm form a membrane-associated biosynthetic complex. We propose that the formation of a membrane complex could serve as a mechanism to ensure the fidelity of CβG biosynthesis by coordinating their synthesis with the transport and modification.

IMPORTANCE

In this study, we analyzed the interaction and localization of the proteins involved in the synthesis, transport, and modification of *Brucella abortus* cyclic β-1,2-glucans (CβG), which play an important role in the virulence and interaction of *Brucella* with the host. We demonstrate that these proteins interact, forming a complex located mainly at the cell poles; this is the first experimental evidence of the existence of a multienzymatic complex involved in the metabolism of osmoregulated periplasmic glucans in bacteria and argues for another example of pole differentiation in *Brucella*. We propose that the formation of this membrane complex could serve as a mechanism to ensure the fidelity of CβG biosynthesis by coordinating synthesis with the transport and modification.

Osmoregulated periplasmic glucans (OPGs) are cyclic, branched cyclic, or branched linear oligosaccharides present in the periplasm of certain Gram-negative bacteria. Common features of these oligosaccharides are the presence of glucose as the sole sugar constituent and the regulation of their synthesis by the osmolarity of the growth milieu. *Agrobacterium*, *Rhizobium*, *Sinorhizobium*, and *Brucella* species synthesize cyclic OPGs consisting of a cyclic chain of 17 to 25 glucose residues linked in β-1,2 glycosidic bonds and substituted with sn-1-phosphoglycerol, succinic acid, methylmalonic acid, or a combination of them (1–3).

Cyclic β-1,2-glucan synthase (Cgs), the enzyme responsible for the synthesis of cyclic β-1,2-glucans (CβG), is present in a restricted number of symbiotic or pathogenic bacteria, most of them belonging to the *Alphaproteobacteria* group, in which CβG are a symbiosis or virulence factor required for successful host interaction (4–6). In *Brucella abortus*, the etiological agent of bovine brucellosis, it has been shown that the synthesis and transport of CβG to the periplasmic space play an important role in virulence (7–9). CβG plays a major role in circumventing host cell defense controlling vacuole maturation, avoiding lysosome fusion, and allowing *Brucella* to reach an endoplasmic reticulum-derived vacuole permissive for bacterial replication (4). Additionally, *Brucella* CβG can be used to enhance cellular immunity by activation of human and mouse dendritic cells (10).

Brucella abortus Cgs is a 320-kDa (2,867-amino-acid-residue) polytopic integral inner membrane protein with six transmembrane segments (TMSs) and the amino and carboxy terminus located on the cytoplasm (11). Cgs itself acts as a protein intermediate and catalyzes the four enzymatic reactions required for the synthesis of CβG. The first glucose is transferred from UDP-glucose to a not-yet-identified amino acid residue of the protein (initiation reaction). Successive glucoses are then transferred from UDP-glucose to the protein-bound glucose, thus elongating a linear polyglucose chain (elongation reaction) linked to the protein.

Received 26 January 2015 **Accepted** 22 February 2015

Accepted manuscript posted online 2 March 2015

Citation Guidolin LS, Morrone Seijo SM, Guaimas FF, Comerci DJ, Ciocchini AE. 2015. Interaction network and localization of *Brucella abortus* membrane proteins involved in the synthesis, transport, and succinylation of cyclic β-1,2-glucans. J Bacteriol 197:1640–1648. doi:10.1128/JB.00068-15.

Editor: P. J. Christie

Address correspondence to Diego J. Comerci, dcomerci@iibintech.com.ar, or Andrés E. Ciocchini, aciocchini@iibintech.com.ar.

Supplemental material for this article may be found at http://dx.doi.org/10.1128/JB.00068-15.

doi:10.1128/JB.00068-15

The initiation and elongation reactions are catalyzed by the Cgs glycosyltransferase domain (amino acid residues 475 to 818) (12). The glucose-removing activity catalyzed by the β-1,2-glucooligosaccharide phosphorylase domain (Cgs residues 1545 to 2867) counteracts the Cgs elongation reaction, thus controlling the length of the β-1,2-glucoologosaccharide protein-linked intermediate (13). The cyclization reaction catalyzed by the Cgs region from positions 991 to 1544 puts an end to the balance between the elongation and phosphorolysis reactions, the linear β-1,2-glucooligosaccharide protein-linked intermediate is cyclized, and CβG (with the appropriate ring size) are released from the protein to the cytoplasm (14). Once in the cytoplasm, CβG are transported to the periplasm by the cyclic glucan transporter Cgt, an ABC transporter of 66 kDa with six predicted TMSs (9). During transport or once they have reached the periplasmic space, a fraction of the CβG are substituted with *O*-succinyl residues, which confer on cyclic β-1,2-glucans an anionic character. This modification of CβG is catalyzed by the succinyltransferase Cgm, an integral inner membrane protein of 43 kDa with nine predicted TMSs (3).

Biosynthesis of CβG is predicted to require strict coordination of the initiation, elongation, phosphorolysis, and cyclization reactions as well as of its export to the periplasm and succinylation. One putative mechanism to maintain the fidelity of polysaccharide biosynthesis is to contain the essential machinery within a membrane-associated biosynthetic complex, and this is how such systems are typically viewed. However, few studies have actually established the existence of protein complexes in the assembly of complex bacterial polysaccharides. The existing information is restricted to capsular polysaccharides and *O*-polysaccharides synthesized by different pathways (15–19). For OPG biosynthesis, current models envisage the formation of multienzyme complexes where the enzymes necessary for backbone synthesis, transport, and backbone modification could work coordinately (1, 2), but to date there is no experimental evidence for the formation of such complexes.

The goal of this study was to examine the potential protein-protein interactions and the localization of the proteins required for *B. abortus* CβG metabolism. Using bacterial two-hybrid (BACTH) and coimmunoprecipitation (Co-IP) strategies, we obtained evidence of homotypic and heterotypic protein-protein interactions among Cgs, Cgt, and Cgm, creating a membrane-located protein complex dedicated to cyclic β-1,2-glucan biosynthesis, transport, and succinylation. Single-cell fluorescence microscopy analysis in *Brucella* demonstrated that these proteins are focally distributed in the membrane, particularly at the cell poles.

MATERIALS AND METHODS

Bacterial strains and growth conditions. Bacterial strains used in this work are listed in Table S1 in the supplemental material. *E. coli* strains were grown in Luria-Bertani (LB) broth (20) at 37°C, unless otherwise indicated. When necessary, medium was supplemented with 50 to 100 μg/ml ampicillin (Amp), 25 to 50 μg/ml kanamycin (Km), 2 μg/ml tetracycline (Tet), 20 μg/ml chloramphenicol (Cm), and 0.5 to 1 mM isopropyl-β-D-1-thiogalactopyranoside (IPTG). *B. abortus* strains were grown in tryptic soy broth (TSB) (Difco/Becton-Dickinson, Sparks, MD) at 37°C. If necessary, TSB was supplemented with 50 μg/ml Amp, 50 μg/ml Km, 20 μg/ml Cm, and/or 5 μg/ml nalidixic acid (Nal). All work with live *B. abortus* was performed in a biosafety level 3 laboratory facility at Universidad Nacional de San Martín.

Plasmid construction and mutagenesis. Plasmids and primers used in this work are listed in Tables S2 and S3 in the supplemental material, respectively. PCRs were performed with *Pfu* polymerase (Promega) and *B. abortus* 2308 genomic DNA or the appropriate plasmids as the templates. For construction of the plasmids used in the BACTH analysis, PCRs were performed with forward and reverse primers containing an XbaI and a BamHI site, respectively. The amplified DNA fragments were digested with XbaI and BamHI and ligated to BACTH vectors (pKT25, pKNT25, pUT18, and pUT18C) digested with the same restriction enzymes. The expression of the corresponding fusion proteins was analyzed in *E. coli* K-12 XL1-Blue MRF′ or DH5α by Western blotting using a specific polyclonal antiserum against CyaA.

For generation of the CgsΔcoil deletion mutant, two DNA fragments flanking the coiled-coil sequence were amplified by PCR using the primer pairs pCgsL4Fw/pCgsB and pCgsC/pCgsW476Rv. After annealing of both DNA fragments (primers pCgsB and pCgsC were designed to partially overlap), the resulting fragment was amplified by PCR using the primers pCgsL4Fw and pCgsW476Rv. Then, the XbaI/SfiI DNA fragment of *cgs* in pKNT25Cgs was replaced with the equivalent mutated fragment to generate pKNT25CgsΔcoil.

The *E. coli mdoC mdoG mdoH mdoB* mutant (*E. coli* Δ*mdo*) and *B. abortus* 2308 *cgs* mutant (*B. abortus* Cgs08) were constructed as described in the supplemental material.

For pKNTCgs-6×His and pKNTCgsΔcoil-6×His plasmid construction, pKNT25 was digested with EcoRI and ClaI, treated with T4 DNA polymerase (New England BioLabs), and religated, generating plasmid pKNT. Then, *cgs* or *cgs*Δcoil was amplified with primers pCgsL4Fw and pCgs-6×HisRv and cloned into the XbaI/BamHI sites of pKNT.

For pCgt-3×FLAG plasmid construction, Cgt was amplified by PCR with pCgtS2BamHIFw/pCgtV598*Spe*IRv primers and cloned into BamHI/SpeI sites of pLF, yielding pLF-Cgt. Then, KpnI/SacI fragment of pLF-Cgt was cloned into pBBR1-MCS3, yielding pCgt-3×FLAG.

The genes coding for the fluorescent proteins enhanced yellow fluorescent protein (EYFP), mCherry, and enhanced cyan fluorescent protein (ECFP) were amplified by PCR using the primers pFP*Spe*IFw and pFP*Xba*IRv and the plasmids pEYFP-C1, pmCherry-C1, and pECFP-C1 (Clontech Laboratories) as the template. The resulting DNA fragments were cloned into the SpeI/XbaI sites of pTFC, yielding pTrc-EYFP, pTrc-mCherry, and pTrc-ECFP. Cgs was amplified by PCR with primers pCgsPro2BamHIFw and pCgsGln2867*Spe*IRv, Cgm was amplified with pCgmV2BamHIFw and pCgmR392*Spe*IRv, and Cgt was amplified with pCgtBamHIS2Fw and pCgtV598LK1*Spe*IRv. The amplified DNA fragments were digested with BamHI/SpeI and ligated to the corresponding plasmids digested with the same restriction enzymes, yielding pTrc-CgsEYFP, pTrc-CgmmCherry, pTrc-CgtEYFP, and pTrc-CgtECFP. The XhoI/SacI DNA fragments of pTrc-EYFP and pTrc-CgsEYFP were subcloned into vector pRH004 digested with the same enzymes in the opposite direction of the *lac* promoter, yielding plasmids pRHY and pRHY-Cgs, respectively. In an analog way, XhoI/SacI DNA fragments of pTrc-ECFP, pTrc-CgtECFP, and pTrc-CgtEYFP were subcloned into pRH004 yielding pRHB, pRHB-Cgt, and pRHY-Cgt. For microscopy analysis, the indicated plasmids were introduced into *B. abortus* 2308 by biparental mating using the *E. coli* S17-λpir strain. To assess the functionality of Cgs and Cgm proteins, each construct was introduced into the corresponding mutant strain (*B. abortus* Cgs08 or *B. abortus* Cgm08).

BACTH analysis. BACTH analysis was performed using the bacterial adenylate cyclase two-hybrid system kit (Euromedex), according to the manufacturer's instructions. In this system the two proteins of interest are fused to complementary fragments (T25 and T18) of the catalytic domain of *Bordetella pertussis* adenylate cyclase (CyaA) and coexpressed in an *E. coli cyaA* reporter strain (BTH101). Interaction between the two proteins results in functional complementation of T18 and T25, restoring the synthesis of cAMP and subsequently activation of the *lac* operon (21). Chemically competent *E. coli* BTH101 (*cya*) cells were cotransformed with plasmids expressing the appropriate T18 and T25 fusion proteins, plated on LB agar supplemented with 40 μg/ml 5-bromo-4-chloro-3-indolyl-β-D-galactopyranoside and 0.5 mM IPTG, and incubated for 36 to 48 h at 30°C

until blue/white colonies were observed. For β-galactosidase activity assays, mid-exponential-phase bacteria were induced with 0.8 mM IPTG and grown overnight at 28°C and 250 rpm. Assays were performed as previously described (22), and enzymatic activity (in Miller units) was calculated as follows: $\{[OD_{420} - (1.75 \times OD_{550})]/(t \times OD_{600} \times \text{volume in ml})\} \times 1{,}000$, where OD is optical density at the indicated wavelength (in nanometers) and t is the time of reaction in minutes. A protein interaction was considered positive when the β-galactosidase activity measured was at least three times higher than the background levels measured for the corresponding negative controls.

Preparation of total membrane fractions. An *E. coli* Δ*mdo* strain harboring the indicated plasmids was grown in 2× YT broth (20), supplemented with the appropriate antibiotics, at 37°C and 250 rpm. At mid-exponential phase, cultures were induced with 1 mM IPTG and grown overnight at 28°C and 250 rpm. Cells were harvested and the total membrane fractions were obtained as previously described (23). Resulting total membrane fractions were resuspended in 750 mM 6-aminocaproic acid, 50 mM bis-Tris (pH 7.0) (ACA buffer) using a glass/Teflon tissue homogenizer. Protein concentration was determined by the method of Lowry et al. (24) using bovine serum albumin as standard. In the case of *B. abortus*, membrane fractions were resuspended in 30 mM Tris-HCl (pH 7.6), 150 mM NaCl, 1 mM EDTA, and 1 mM phenylmethanesulfonyl fluoride (PMSF).

Coimmunoprecipitation analysis. Total membrane fractions were resuspended in ACA buffer, 2% dodecyl β-D-maltoside (DDM), and 1 mM PMSF (IP buffer) at a final concentration of 5 mg/ml and incubated for 2 h until solubilization of membrane proteins. Samples were centrifuged at 20,000 × *g* for 30 min at 4°C, and the solubilized proteins were incubated for 1 h with G protein-coupled magnetic beads (New England BioLabs) to remove nonspecifically binding materials (preclearing). Then, the samples were incubated for 18 h with rabbit polyclonal anti-6×His (Rockland) or rabbit polyclonal anti-3×FLAG (Sigma-Aldrich) antibodies, and G protein-coupled magnetic beads were added and incubated for two additional hours. Finally, the beads were washed 3 times with IP buffer, and bound materials were eluted by boiling for 5 min at 100°C in Laemmli sample buffer containing 0.5× IP buffer.

Western blotting. Whole-cell extracts of the corresponding strains or Co-IP samples were subjected to 8 or 10% sodium dodecyl sulfate-polyacrylamide gel electrophoresis (SDS-PAGE) and transferred by electroblotting to nitrocellulose (Millipore) or, for Co-IP, polyvinylidene difluoride membranes (Amersham). Immunoblotting was performed with a specific rabbit polyclonal anti-6×His (Rockland), mouse polyclonal anti-CyaA or mouse monoclonal anti-3×FLAG M2 (Sigma-Aldrich) antibodies. Bound antibodies were detected by using horseradish peroxidase-conjugated goat anti-mouse or anti-rabbit Ig antibodies and the SuperSignal West Pico chemiluminescent substrate detection reagents (Thermo Scientific) according to the manufacturer's instructions. In some cases, IRDye secondary anti-mouse or anti-rabbit Ig antibodies (Li-Cor, Inc.) were used and detection was performed using the Odyssey Imaging System (Li-Cor, Inc.).

Microscopy analysis. Exponential-phase cultures of *B. abortus* strains expressing the various fluorescent fusion proteins were placed on a microscope slide that was layered with a pad of 1% agarose in phosphate-buffered saline (PBS) as previously described (25, 26). For image acquisition, samples were examined on an IX81 microscope with an Olympus FV1000 confocal module (60× PLAPO objective, numerical aperture [NA] of 1.42). For each observation under the microscope, at least three fields were randomly selected for analysis. Images were processed with the Image J program (NIH, Bethesda, MD).

Computer analysis. The Coils program (27) was used to predict coiled-coil structures within the amino acid sequence of the proteins.

RESULTS

Analysis of Cgs, Cgt, and Cgm interactions. (i) Analysis of the interactions by BACTH assays. To investigate the interactions among Cgs, Cgt, and Cgm *in vivo*, a BACTH analysis was performed (21, 28). For this analysis, the T18 and T25 complementary domains of the *Bordetella pertussis* adenylate cyclase (CyaA) catalytic domain were fused at the carboxy terminus of Cgs, Cgt, and Cgm, and the expression of the six fusion proteins was assessed in *E. coli* BTH101 by Western blotting (see Fig. S1A in the supplemental material). All these carboxyl-terminal fusion constructs were functional, based on production of CβG in *E. coli* (see Fig. S1B in the supplemental material). High levels of β-galactosidase activity were observed when the fusion protein pairs Cgs-T18/Cgs-T25, Cgt-T18/Cgt-T25, and Cgm-T18/Cgm-T25 were coexpressed, whereas no functional complementation was detected when Cgs, Cgt, and Cgm fused to T25 or T18 were coexpressed with the control plasmids, indicating that the observed interactions are specific (Fig. 1A). These results suggest that Cgs, Cgt, and Cgm may form dimers or higher-order multimers. Additionally, the existence of heterotypic interactions among the three proteins was analyzed. As shown in Fig. 1B, high values of β-galactosidase activity with respect to the controls were observed with the protein pairs Cgt/Cgm, Cgs/Cgt, and Cgs/Cgm. Addi-

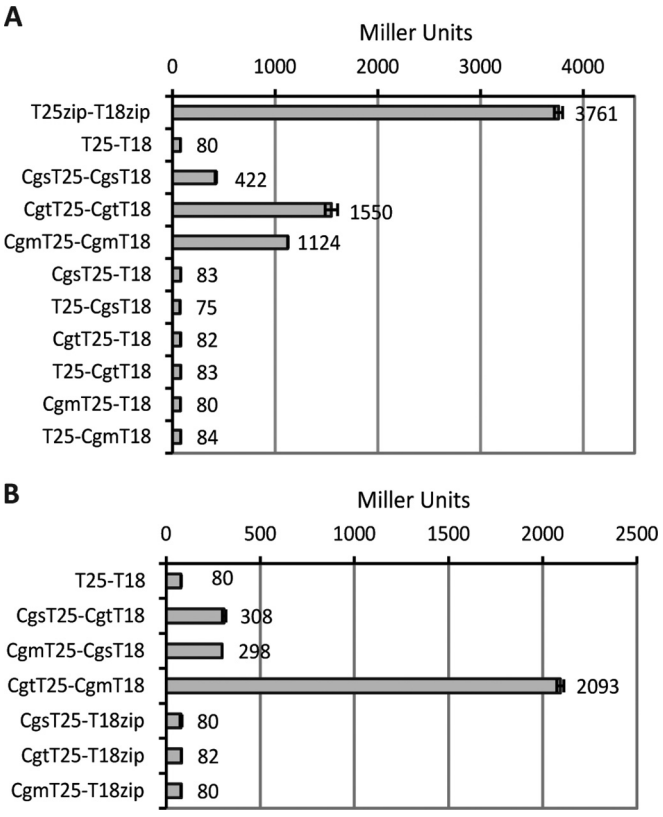

FIG 1 Bacterial two-hybrid (BACTH) analysis of selected pair constructs of Cgs, Cgt, and Cgm. (A) Homotypic interactions. (B) Heterotypic interactions. T18 and T25 domains of CyaA were fused to the carboxy termini of Cgs, Cgt, and Cgm. The efficiency of functional complementation between the indicated hybrid proteins was quantified by measuring the β-galactosidase activity in *E. coli* BTH101 cells harboring the corresponding plasmids as described in Materials and Methods. The activity value for the BACTH positive control (T18-zip + T25-zip) is shown only in panel A. Results are representative of three independent experiments. Error bars indicate the standard deviations of the measurements. A protein interaction was considered positive when the β-galactosidase activity was at least three times higher than the background levels for the corresponding negative controls.

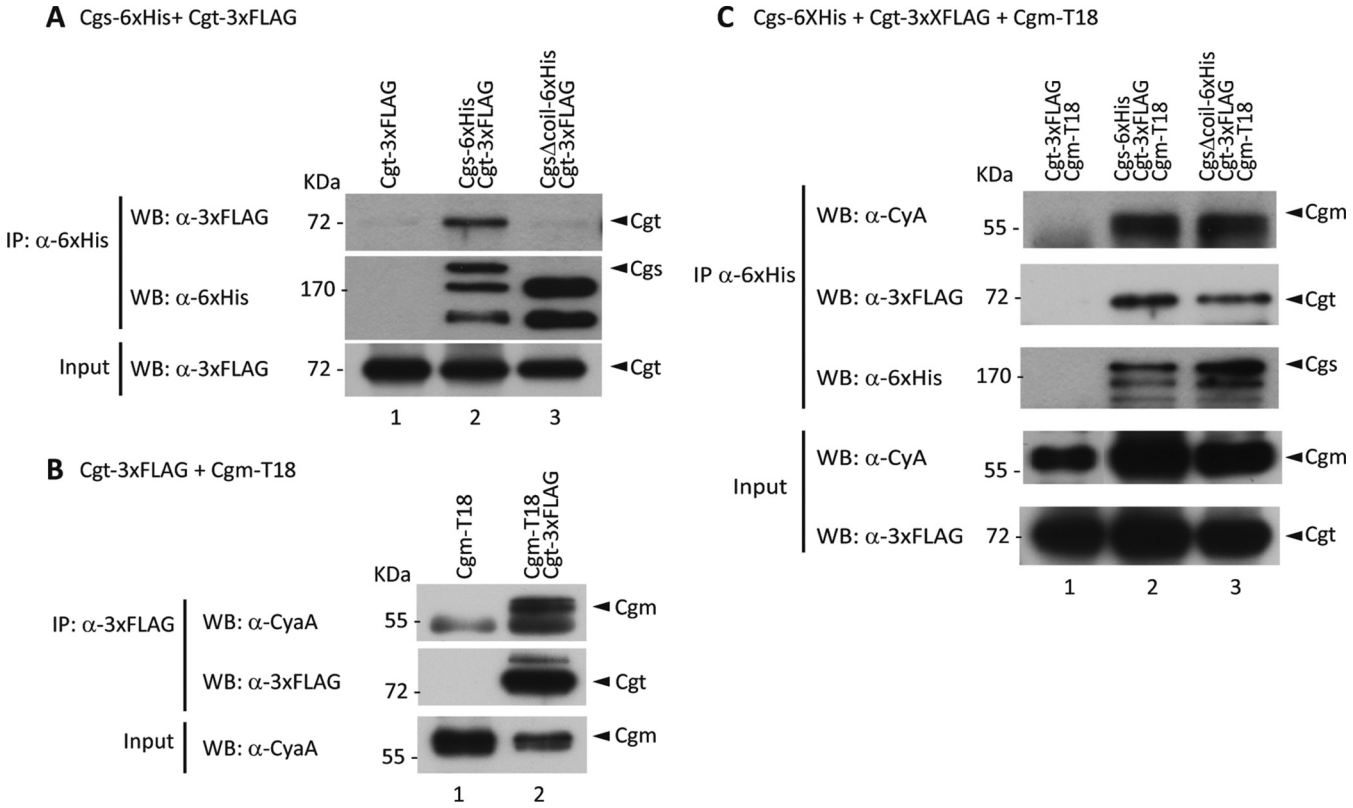

FIG 2 Coimmunoprecipitation (Co-IP) analysis. Total membrane fractions of *E. coli* Δ*mdo* expressing the indicated fusion proteins were solubilized in 2% DDM and subjected to immunoprecipitation (IP) with the indicated antibodies. The immunocomplexes were analyzed by Western blotting (WB). (A) Co-IP analysis of protein extracts from *E. coli* Δ*mdo* expressing Cgt-3×FLAG (lane 1), Cgt-3×FLAG/Cgs-6×His (lane 2), or Cgt-3×FLAG/CgsΔcoil-6×His (lane 3). Immunoprecipitation was performed with rabbit anti-6×His polyclonal antibodies. (B) Co-IP analysis of protein extracts from *E. coli* Δ*mdo* expressing Cgm-T18 (lane 1) or Cgt-3×FLAG/Cgm-T18 (lane 2). Immunoprecipitation was performed with rabbit anti-3×FLAG polyclonal antibodies. (C) Co-IP analysis of protein extracts from *E. coli* Δ*mdo* coexpressing Cgt-3×FLAG/Cgm-T18 (lane 1), Cgt-3×FLAG/Cgm-T18/Cgs-6×His (lane 2) or Cgt-3×FLAG/Cgm-T18/CgsΔcoil-6×His (lane 3). Immunoprecipitation was performed with rabbit anti-6×His polyclonal antibodies. The bands observed just below the Cgm migration position (Fig. 2B and C, top panels) correspond to cross-reactivity of the secondary anti-mouse antibody with the heavy chains of rabbit immunoglobulins used to immunoprecipitate the protein complex.

tionally, the same interactions were detected when the various bait-and-prey combinations, for both homotypic and heterotypic interactions, were reversed (data not shown). Taken together, these results indicate that Cgs, Cgt, and Cgm can form both homotypic and heterotypic interactions, which is consistent with the formation of a membrane complex for CβG biosynthesis.

(ii) Analysis of the interactions by Co-IP. To confirm the results obtained by BACTH analysis, pairwise and triple combinations of Cgs, Cgt, and Cgm were assessed for interaction by a coimmunoprecipitation (Co-IP) strategy. Cgs-6×His, Cgt-3×FLAG, and Cgm-T18 were coexpressed in the *E. coli* Δ*mdo* strain lacking the genes required for the synthesis of linear OPGs, and the synthesis of CβG was analyzed by thin-layer chromatography (TLC). The expression of Cgs, Cgt, and Cgm in this strain allowed us to analyze the synthesis of CβG by TLC without the interference of linear OPGs produced by *E. coli*. Figure S2 in the supplemental material shows that coexpression of the three fusion proteins resulted in the synthesis of neutral and anionic CβG, indicating that the three fusion proteins were functional.

Incubation of solubilized membrane fractions of *E. coli* Δ*mdo* coexpressing Cgs-6×His/Cgt-3×FLAG with anti-6×His antibodies resulted in coimmunoprecipitation of Cgt (Fig. 2A, lane 2). Cgt was not detected in cells expressing Cgt-3×FLAG alone, indicating that the immunoprecipitation of Cgt is specific (Fig. 2A, lane 1). When solubilized membranes of cells that coexpress Cgt-3×FLAG/Cgm-T18 were incubated with anti-3×FLAG antibodies, Cgm coimmunoprecipitated with Cgt (Fig. 2B, lane 2). Coimmunoprecipitation of Cgt was not observed in cells that express only Cgm-T18 (Fig. 2B, lane 1). Attempts to coexpress Cgs and Cgm were unsuccessful, indicating some instability of the proteins under these conditions. However, we were able to coexpress the three proteins. Solubilized membranes of cells that coexpressed Cgs-6×His, Cgt-3×FLAG, and Cgm-T18 were incubated with anti-6×His antibodies, resulting in Cgt and Cgm coimmunoprecipitation (Fig. 2C, lane 2). Coimmunoprecipitation of Cgt and Cgm with anti-6×His antibodies was not detected in cells coexpressing Cgt-3×FLAG/Cgm-T18 (Fig. 2C, lane 1), demonstrating that the immunoprecipitation of Cgt and Cgm is specific. Taken together, these data corroborate the results previously obtained by BACTH analysis indicating that Cgs, Cgt, and Cgm are able to form a multienzymatic membrane complex.

Analysis of Cgs regions required to maintain the protein interactions. To identify the Cgs region/s involved in the protein-protein interactions, different carboxyl-terminal truncated Cgs variants were obtained by deleting the cytoplasmic domains from the carboxy terminus and preserving as many TMSs as possible

(Fig. 3A; also, see Fig. S1C in the supplemental material). These truncated proteins were fused to the T18 domain of CyaA, and their interactions with Cgs-T25, Cgt-T25 and Cgm-T25 were analyzed by BACTH. As shown in Fig. 3B, the minimal region of Cgs required for maintaining homotypic interactions is the region from positions 4 to 871. The minimal region of Cgs necessary to maintain the heterotypic interactions with Cgt and Cgm was the region from positions 4 to 475. The interaction of Cgs, Cgt, and Cgm with the truncated Cgs versions (in particular with the truncated proteins Cgs1552-T18, Cgs999-T18, and Cgs871-T18) resulted in higher β-galactosidase activity levels than interaction with full-length Cgs, suggesting that the carboxyl-terminal region adds some instability to the constructs. In this sense, a higher stability of Cgs truncated proteins in comparison with full-length Cgs was consistently observed by immunoblotting (see Fig. S1C in the supplemental material).

The functional role of the amino-terminal region of Cgs (positions 1 to 418) is not known and this region exhibit no similarity to proteins with known function; although, previous *in silico* sequence and structural analyses allowed us to predict in this region a putative protein-protein interaction module (12). Detailed *in silico* sequence analysis of this region with the program Coils (27) predicted the presence of a coiled-coil domain of four heptads between amino acid residues 185 and 215 (Fig. 3A). A Cgs mutant with a deletion of this coiled-coil domain (CgsΔcoil) was generated. This mutant was active for the synthesis of CβG, producing CβG with a high degree of polymerization (DP) and expressed properly in *E. coli* (see Fig. S3 in the supplemental material). As shown in Fig. 3C, no interaction of this mutant with Cgs, Cgt, and Cgm was observed by BACTH analysis. A similar result was obtained for the pair CgsΔcoil-6×His/Cgt-3×FLAG by Co-IP (Fig. 2A, lane 3), indicating that the coiled-coil domain is required for Cgs-Cgt interaction. However, analysis of the interactions by Co-IP in cells coexpressing CgsΔcoil-6×His/Cgt-3×FLAG/Cgm-T18 resulted in the coimmunoprecipitation of Cgt and Cgm when the solubilized proteins were incubated with anti-6×His antibodies (Fig. 2C, lane 3), indicating that other Cgs regions besides the coiled-coil domain may also be important to sustain the interactions when the three proteins are expressed simultaneously. Therefore, the coiled-coil domain contained in the amino-terminal region of Cgs is necessary but not sufficient to maintain the interactions.

Overall, these results indicate that the amino-terminal region of Cgs (residues 1 to 418) constitutes a noncatalytic domain required for homotypic and heterotypic interactions.

Localization of Cgs, Cgt, and Cgm proteins in *Brucella abortus*. In order to analyze the subcellular localization of Cgs, Cgt, and Cgm and therefore the complex that they form, the three proteins were fused to different fluorescent proteins, expressed in *B. abortus*, and analyzed by fluorescence microscopy. Cgs and Cgm were fused at the carboxy terminus to EYFP and mCherry, respectively. For expression of Cgt fused to different fluorescent proteins, a linker of six amino acid residues was added between the proteins to enable proper expression. The expression of the fluorescent fusion proteins was analyzed by SDS-PAGE and in-gel fluorescence detection, as described in Materials and Methods. As shown in Fig. S4A in the supplemental material, all the fusion proteins have the expected molecular weight and were correctly detected in the membrane fraction. Additionally, Cgs-EYFP and

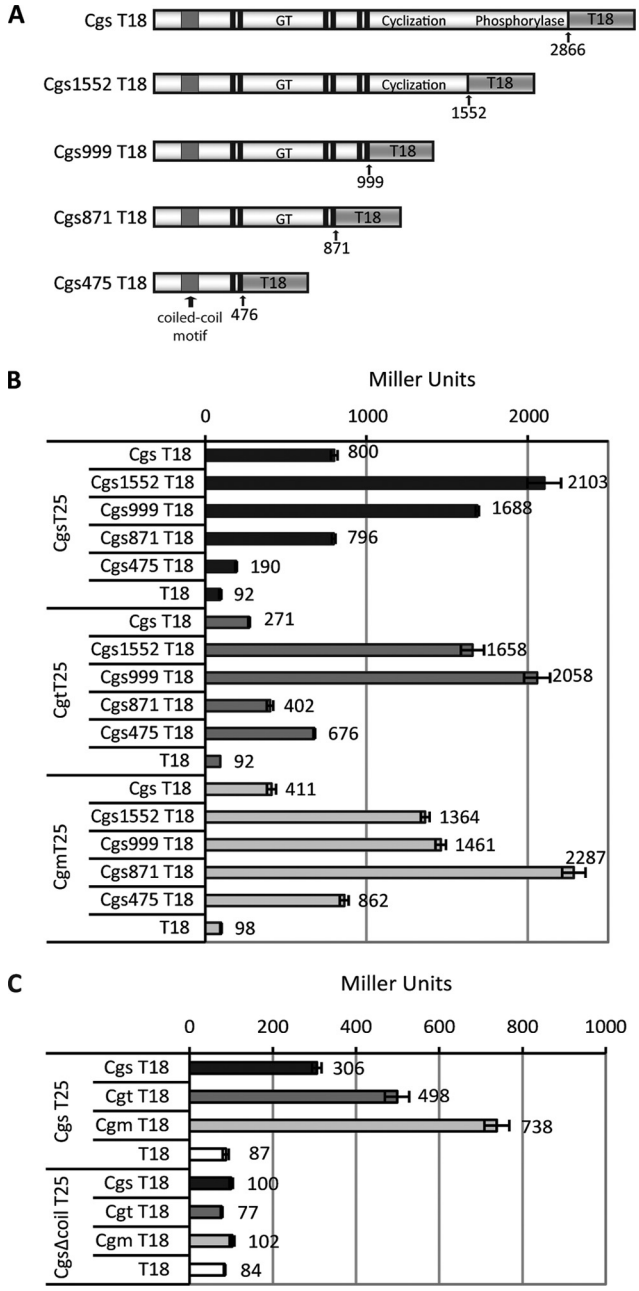

FIG 3 Analysis of Cgs regions involved in the protein-protein interactions. (A) Schematic representation of Cgs and carboxyl-terminally truncated proteins. Arrows and numbers indicate the amino acid positions of Cgs where the T18 domain was fused. Cgs truncated proteins were named with the position number of the last amino acid residue conserved in the truncated protein. Black rectangles represent the TMSs. Carboxyl-terminal deletions were performed in order to maintain as many TMSs as possible. The mutant Cgs1552 lacks the phosphorylase domain. Cgs999 lacks the phosphorylase and cyclization domains. Cgs871 conserves the first and second (glycosyltransferase) cytosolic domains. Cgs471 conserves only the first cytosolic domain with the first and second TMSs. (B) BACTH analysis of Cgs-T25, Cgt-T25, or Cgm-T25 when coexpressed with the carboxyl-terminal truncated versions of Cgs fused to the T18 domain. (C) BACTH analysis of the Cgs coiled-coil deletion mutant. The efficiency of functional complementation of the selected pair constructs was quantified by measuring the β-galactosidase activity. Results are representative of three independent experiments. Error bars indicate standard deviations. Under the same assay conditions, the positive control [strain BTH101(pKT25-zip, pUT18C-zip)] yielded a value of 4,500 Miller units.

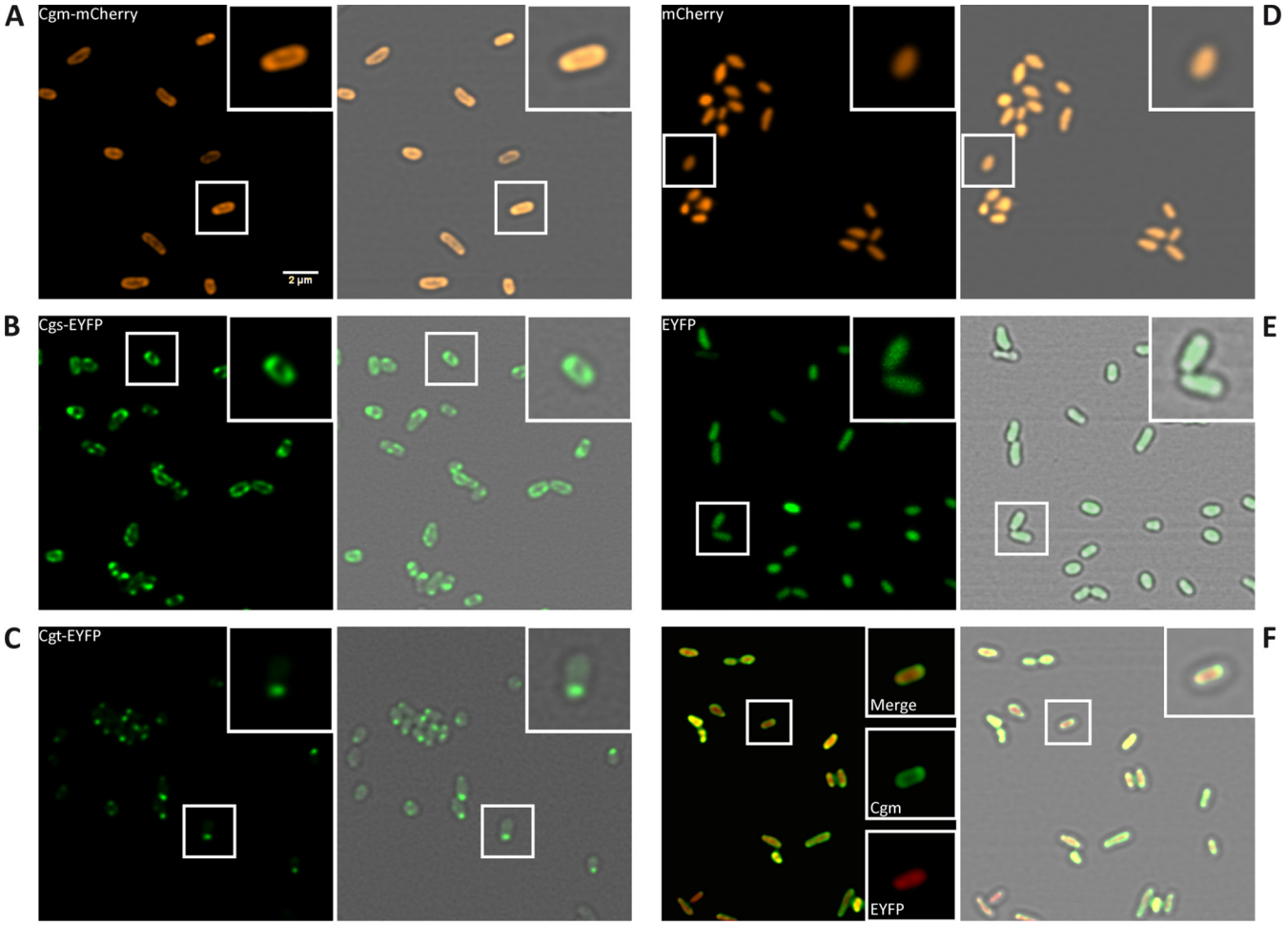

FIG 4 Fluorescence microscopy analysis of Cgs, Cgt, and Cgm. Exponential-phase cultures of *Brucella abortus* 2308 expressing Cgm-mCherry (A), Cgs-EYFP (B), Cgt-ECFP (C), mCherry (D), or EYFP (E) or coexpressing Cgm-mCherry/EYFP (F) were placed on a microscope slide layered with a pad of 1% agarose in PBS. The subcellular localization of proteins was analyzed by confocal fluorescence microscopy. Panels on the right show the superposition of white-field and fluorescence microscopy images.

Cgm-mCherry fusion proteins were active in complementation assays (see Fig. S4B in the supplemental material).

Fluorescence microscopy analysis showed that Cgm-mCherry is mostly distributed throughout the *Brucella* membrane, with a slight accumulation at both cell poles (Fig. 4A). It is interesting that, despite the small size of *Brucella*, fluorescent signals at the plasma membrane and the cytoplasm are clearly contrastable, as observed when Cgm-mCherry is coexpressed with soluble EYFP (Fig. 4F). For Cgs-EYFP we observed that the fluorescence signal is mostly concentrated in foci of high fluorescence intensity and less extensively distributed in the plasma membrane. In most cases, at least one of these foci was located at the cell poles (Fig. 4B). For Cgt-EYFP and Cgt-ECFP, both fusion proteins displayed the same localization pattern and almost all the fluorescence signal has a polar accumulation; in many cases, there was only one focus of high fluorescence intensity at one cell pole, but in some cases, there were two foci, one at each cell pole (Fig. 4C; also data not shown). As expected, mCherry, EYFP, and ECYFP displayed a cytoplasm distribution independently of the expression vector used (Fig. 4D and E; also, see Fig. S5 in the supplemental material).

Coexpression experiments with the pair Cgt-ECFP/Cgs-EYFP revealed a clear colocalization of both signals with a distribution pattern similar to that observed with Cgs alone, suggesting that Cgt is recruited to Cgs accumulation foci (Fig. 5A). When Cgm-mCherry was coexpressed with Cgs-EYFP, we observed for each protein the same distribution pattern of fluorescence that it had when expressed separately, showing the superposition of fluorescence signals in foci of Cgs accumulation (Fig. 5B). Finally, coexpression of Cgm-mCherry with Cgt-EYFP resulted in the same distribution of fluorescence as when the proteins were expressed separately, with some superposition of the fluorescence signals, since Cgm is distributed all over the membrane (Fig. 5C).

Taken together, these results are consistent with the interactomic data indicating that Cgs, Cgt, and Cgm form a CβG biosynthetic complex in the plasma membrane of *Brucella* located preferentially at the cell poles.

DISCUSSION

Biosynthesis of CβG is predicted to require strict coordination of the initiation, elongation, phosphorolysis, and cyclization reactions as well as for its export to the periplasm and succinylation. One putative mechanism to maintain the fidelity of polysaccha-

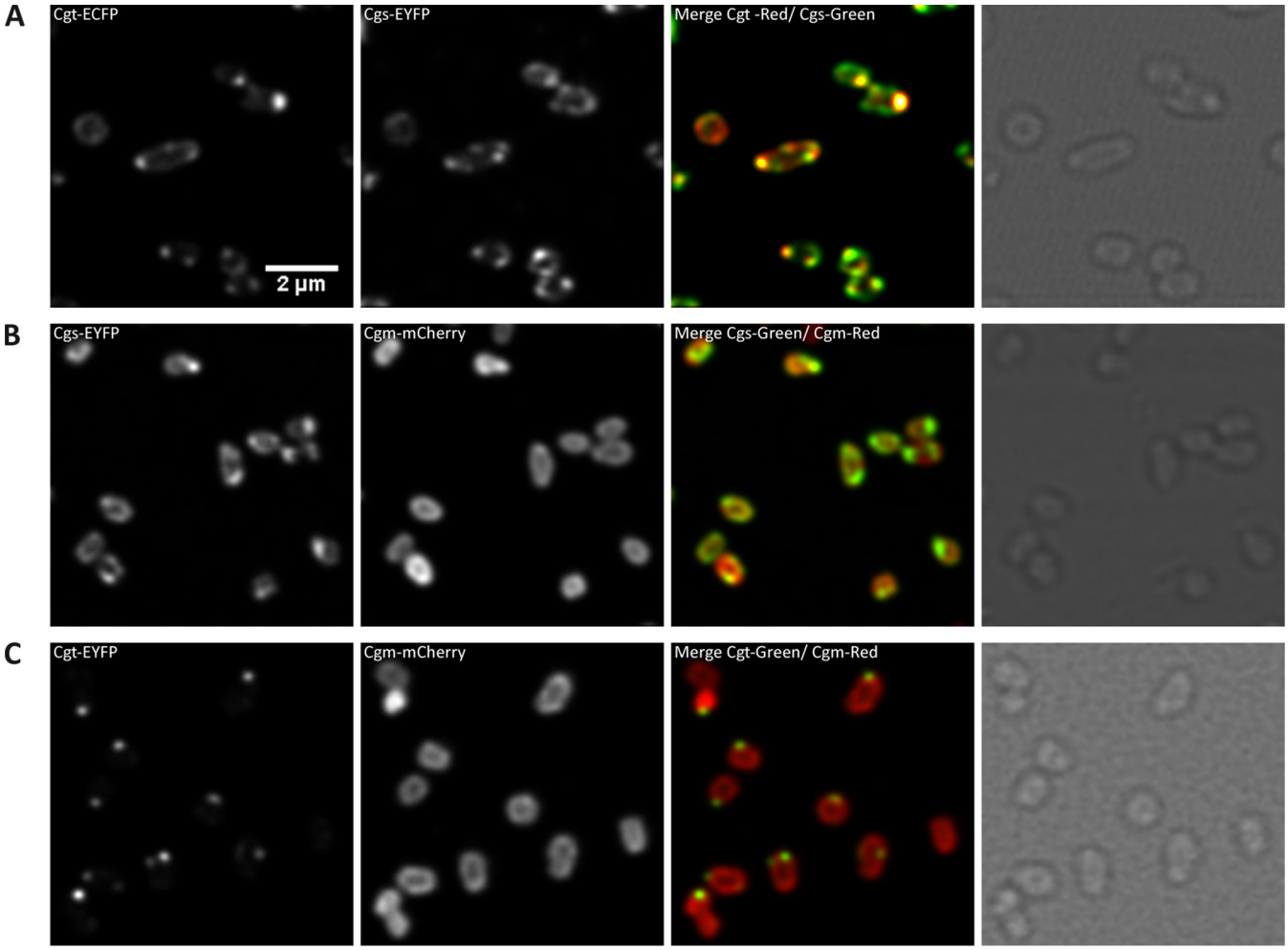

FIG 5 Fluorescence microscopy analysis of pairwise combinations of Cgs, Cgt, and Cgm. Exponential-phase cultures of *Brucella abortus* 2308 coexpressing Cgt-ECFP/Cgs-EYFP (A), Cgt-EYFP/Cgm-mCherry (B), or Cgs-EYFP/Cgm-mCherry (C) were placed on a microscope slide layered with a pad of 1% agarose in PBS. The subcellular localization of proteins was analyzed by confocal fluorescence microscopy.

ride biosynthesis is to contain the essential machinery within a membrane-associated biosynthetic complex. We hypothesize that the multimodular nature of Cgs, by which all the enzymatic activities required for the synthesis of CβG are contained within the same polypeptide in discrete domains, together with the formation of a Cgs-Cgt-Cgm membrane complex could serve as a mechanism to maintain the fidelity of cyclic β-1,2-glucans biosynthesis and coordinate the synthesis with its transport and modification.

In this work, we used a bacterial two-hybrid system and coimmunoprecipitation techniques to study the interaction network between Cgs, Cgt, and Cgm. Our results indicate that Cgs, Cgt, and Cgm maintain homotypic and heterotypic interactions, demonstrating that these three proteins form a complex in the bacterial membrane responsible for the synthesis, transport, and succinylation of CβG. This complex may contain more than one copy of Cgs, Cgt, and Cgm, as these proteins are able to establish homotypic interactions. Cross-linking and blue-native gel electrophoresis experiments were performed in order to evaluate the stoichiometry of the complex with no satisfactory results, probably due to the high molecular weight of the complex and the high hydrophobicity of the proteins. Alternative experiments are under way to resolve this issue. Analyses carried out with Cgs carboxyl-terminally truncated proteins revealed that the minimal region necessary to maintain Cgs-Cgs interactions is the Cgs region from positions 1 to 871 and that the region from 1 to 476 is the minimal region required for the interaction of Cgs with Cgt and Cgm. Additionally, a coiled-coil motif located between amino acid residues 185 and 215 is required to sustain the interactions of Cgs with Cgt and Cgm as well as with itself, although other regions may also be implicated. As expected, the three proteins displayed a membrane localization by fluorescence microscopy in *Brucella*. While Cgt and Cgs presented a focal distribution, mainly at the cell poles, Cgm seemed to be more homogeneously distributed in the membrane, although a slightly accumulation at the cell poles was also evident. When coexpressed, all three proteins showed regions where colocalization was evident, particularly with Cgs and Cgt. These observations are compatible with the protein-protein interaction results obtained by BACTH and Co-IP, supporting the existence of a Cgs-Cgt-Cgm protein complex in *Brucella*.

On the basis of past work and the evidence presented here, we propose that Cgs is a polyfunctional modular protein in which catalytic and noncatalytic discrete domains can be recognized.

The Cgs region from amino acid residues 1 to 1544 constitutes the minimal region required for catalysis of the initiation, elongation, and cyclization reactions; thus, it is a polyfunctional region by itself in which each reaction is catalyzed by a different discrete domain (14). In this region, we previously identified the glycosyltransferase domain GT-84 (Cgs positions 475 to 818), which catalyzes the initiation and elongation reactions (12), and the cyclization domain (Cgs positions 991 to 1544) (14). The carboxyl-terminal region (residues 1545 to 2867) displays the β-1,2-glucooligosaccharide phosphorylase activity through which Cgs controls the DP of the glucooligosaccharide protein-linked intermediate (13). In this work, we have demonstrated that the amino-terminal region of Cgs (residues 1 to 418) constitutes a noncatalytic domain of Cgs required to maintain the protein-protein interactions with Cgs, Cgt, and Cgm.

In the biosynthesis of CβG, elongation, phosphorolysis, and cyclization reactions occur on the same substrate, which is the nonreducing end of the polyglucose chain linked to the Cgs protein. In Cgs, the presence of multiple functional domains within the same polypeptide ensures that all catalytic activities required for the synthesis of CβG are confined near the substrate and may be one of the mechanisms that allow a proper coordination among the initiation, elongation, phosphorolysis, and cyclization reactions required for the synthesis of CβG. In agreement with this hypothesis and from both *in vitro* and *in vivo* experiments, we previously demonstrated that the carboxyl-terminal phosphorylase domain of Cgs must be part of the same polypeptide chain to be able to catalyze glucan phosphorolysis and hence to control the degree of polymerization of CβG (13). Intraprotein interactions may also occur between distinct domains of Cgs, setting another level of coordination among the different reactions catalyzed by this protein. A piece of evidence supporting this hypothesis is the change in the size of CβG observed in the coiled-coil deletion mutant located at the amino-terminal region of Cgs. This mutant not only is affected in its interaction pattern with Cgs, Cgt, and Cgm but also produces CβG with a high DP, indicating that the CβG size control mechanism is affected (see Fig. S3A in the supplemental material). In agreement with these results, we previously obtained and characterized Cgs mutants with in-frame pentapeptide insertions at positions 160 and 302, flanking the coiled-coil domain identified in this work, that also produced CβG with a high DP (14). These results suggest that the Cgs amino-terminal region may interact with the cyclization and/or phosphorylase domains located at the carboxy terminus, thus allowing the enzyme to acquire a proper spatial conformation suitable for catalysis and control of CβG DP. Transport and succinylation of CβG could be coordinated in an analogous way by the establishment of protein-protein interactions among Cgs, Cgt, and Cgm and thereby through the formation of a protein complex in the inner membrane of the bacteria. Further work will be required to establish the biological importance of Cgs-Cgt-Cgm interactions for the synthesis, transport, and modification of CβG as well as for the intracellular survival and virulence of *Brucella*.

The hypothesis that multienzymatic membrane complexes are implicated in the coordination of the biosynthesis (initiation, elongation, and termination) and transport of *O* polysaccharides and other bacterial polysaccharides is currently being strengthened experimentally (15, 17, 18, 29). Some of these polysaccharides and the lipopolysaccharides (LPS) are important virulence factors in a wide spectrum of bacterial infections. Examples of polysaccharide biosynthetic complexes include those responsible for the synthesis of teichoic acid in *Bacillus subtilis* (18), *E. coli* LPS O9a antigen (15), and the complex responsible for the synthesis of *E. coli* group 2 capsular antigen (17). It was demonstrated that in LPS O9a antigen biosynthesis, the glycosyltransferase activity of WbdA is dependent on protein-protein interactions with WbdD, the terminator enzyme, which recruits the polymerase to a functional complex on the cytoplasmic membrane (15). Recent studies of the glycosyltransferases involved in the synthesis of the K5 capsular polysaccharide have demonstrated that protein-protein interactions were essential for activity. In this large transenvelope complex, the glucuronyltransferase activity of KfiC is dependent on physical association with the *N*-acetylglucosaminyltransferase KfiA (29). Moreover, it has been demonstrated that this complex has a polar localization, consistent with the site where the biosynthesis and export of this polysaccharide occur (17). A working model, where the enzymes necessary for backbone synthesis, transport, and modification could work coordinately in a protein complex in the bacterial inner membrane, has been proposed for the biosynthesis of the linear highly branched *E. coli* OPGs, but until now no experimental evidence has supported this model (1). In this work, we have demonstrated that the three proteins involved in the synthesis, transport, and succinylation of CβG interact, forming a complex located mainly at cell poles of *Brucella* organisms. This is the first experimental evidence of the existence of a multienzymatic complex involved in OPG metabolism.

Brucella organisms are polarized bacteria that grow unidirectionally from the new pole generated after cell division. This growing characteristic generates two different cells after cell division: a mother cell inheriting the old envelope material and a daughter cell having a newly synthesized envelope (30). Recent reports suggest that the polar distribution of certain proteins and the asymmetry of *Brucella* growth have a functional role. Recently described cell cycle progression in *Brucella* highlights the functional relevance for subcellular specific localization in or near cell poles of the chromosome I centromere-binding protein ParB and the RepABC chromosome II partitioning system for chromosome replication and segregation (31). Additionally, the localization of the essential PdhS histidine kinase and its response regulator DivK in the old pole of the cell seems to be important for cell cycle progression (32). In *B. suis*, the polar localization of the BtaE and BmaC adhesins defines an adhesive pole, consistently associated with the new cell pole, suggesting that the new cell pole is functionally differentiated for adhesion to host (26, 33). In this work, we observed that the proteins involved in CβG metabolism, particularly Cgs and Cgt, are located mainly at the cell poles, arguing for another example of pole differentiation in *Brucella*. The location of the complex during the intracellular infection phase as well as whether this location also corresponds to the sites of active CβG biosynthesis, transport, and modification remains to be determined.

ACKNOWLEDGMENTS

This work was supported by grants PICT 2011/1485 and PICT 2014/3359 from Agencia Nacional de Promoción Científica y Tecnológica (ANPCyT), Argentina. L.S.G. and S.M.M.S. are research fellows of Consejo Nacional de Investigaciones Científicas y Técnicas (CONICET), Buenos Aires, Argentina. D.J.C. and A.E.C. are career investigators of CONICET.

We thank Xavier De Bolle for his generous gift of plasmid pRH004.

REFERENCES

1. **Bohin JP.** 2000. Osmoregulated periplasmic glucans in Proteobacteria. FEMS Microbiol Lett **186:**11–19. http://dx.doi.org/10.1111/j.1574-6968.2000.tb09075.x.
2. **Breedveld MW, Miller KJ.** 1994. Cyclic beta-glucans of members of the family Rhizobiaceae. Microbiol Rev **58:**145–161.
3. **Roset MS, Ciocchini AE, Ugalde RA, Inon de Iannino N.** 2006. The Brucella abortus cyclic beta-1,2-glucan virulence factor is substituted with O-ester-linked succinyl residues. J Bacteriol **188:**5003–5013. http://dx.doi.org/10.1128/JB.00086-06.
4. **Arellano-Reynoso B, Lapaque N, Salcedo S, Briones G, Ciocchini AE, Ugalde R, Moreno E, Moriyon I, Gorvel JP.** 2005. Cyclic beta-1,2-glucan is a Brucella virulence factor required for intracellular survival. Nat Immunol **6:**618–625. http://dx.doi.org/10.1038/ni1202.
5. **Dylan T, Ielpi L, Stanfield S, Kashyap L, Douglas C, Yanofsky M, Nester E, Helinski DR, Ditta G.** 1986. Rhizobium meliloti genes required for nodule development are related to chromosomal virulence genes in Agrobacterium tumefaciens. Proc Natl Acad Sci U S A **83:**4403–4407. http://dx.doi.org/10.1073/pnas.83.12.4403.
6. **Puvanesarajah V, Schell FM, Stacey G, Douglas CJ, Nester EW.** 1985. Role for 2-linked-beta-D-glucan in the virulence of Agrobacterium tumefaciens. J Bacteriol **164:**102–106.
7. **Briones G, Inon de Iannino N, Roset M, Vigliocco A, Paulo PS, Ugalde RA.** 2001. Brucella abortus cyclic beta-1,2-glucan mutants have reduced virulence in mice and are defective in intracellular replication in HeLa cells. Infect Immun **69:**4528–4535. http://dx.doi.org/10.1128/IAI.69.7.4528-4535.2001.
8. **Iñón de Iannino N, Briones G, Tolmasky M, Ugalde RA.** 1998. Molecular cloning and characterization of cgs, the Brucella abortus cyclic beta(1-2) glucan synthetase gene: genetic complementation of Rhizobium meliloti ndvB and Agrobacterium tumefaciens chvB mutants. J Bacteriol **180:**4392–4400.
9. **Roset MS, Ciocchini AE, Ugalde RA, Inon de Iannino N.** 2004. Molecular cloning and characterization of cgt, the Brucella abortus cyclic beta-1,2-glucan transporter gene, and its role in virulence. Infect Immun **72:**2263–2271. http://dx.doi.org/10.1128/IAI.72.4.2263-2271.2004.
10. **Martirosyan A, Perez-Gutierrez C, Banchereau R, Dutartre H, Lecine P, Dullaers M, Mello M, Salcedo SP, Muller A, Leserman L, Levy Y, Zurawski G, Zurawski S, Moreno E, Moriyon I, Klechevsky E, Banchereau J, Oh S, Gorvel JP.** 2012. Brucella beta 1,2 cyclic glucan is an activator of human and mouse dendritic cells. PLoS Pathog **8:**e1002983. http://dx.doi.org/10.1371/journal.ppat.1002983.
11. **Ciocchini AE, Roset MS, Inon de Iannino N, Ugalde RA.** 2004. Membrane topology analysis of cyclic glucan synthase, a virulence determinant of Brucella abortus. J Bacteriol **186:**7205–7213. http://dx.doi.org/10.1128/JB.186.21.7205-7213.2004.
12. **Ciocchini AE, Roset MS, Briones G, Inon de Iannino N, Ugalde RA.** 2006. Identification of active site residues of the inverting glycosyltransferase Cgs required for the synthesis of cyclic beta-1,2-glucan, a Brucella abortus virulence factor. Glycobiology **16:**679–691. http://dx.doi.org/10.1093/glycob/cwj113.
13. **Ciocchini AE, Guidolin LS, Casabuono AC, Couto AS, de Iannino NI, Ugalde RA.** 2007. A glycosyltransferase with a length-controlling activity as a mechanism to regulate the size of polysaccharides. Proc Natl Acad Sci U S A **104:**16492–16497. http://dx.doi.org/10.1073/pnas.0708025104.
14. **Guidolin LS, Ciocchini AE, Inon de Iannino N, Ugalde RA.** 2009. Functional mapping of Brucella abortus cyclic beta-1,2-glucan synthase: identification of the protein domain required for cyclization. J Bacteriol **191:**1230–1238. http://dx.doi.org/10.1128/JB.01108-08.
15. **Clarke BR, Greenfield LK, Bouwman C, Whitfield C.** 2009. Coordination of polymerization, chain termination, and export in assembly of the Escherichia coli lipopolysaccharide O9a antigen in an ATP-binding cassette transporter-dependent pathway. J Biol Chem **284:**30662–30672. http://dx.doi.org/10.1074/jbc.M109.052878.
16. **Kos V, Whitfield C.** 2010. A membrane-located glycosyltransferase complex required for biosynthesis of the D-galactan I lipopolysaccharide O antigen in Klebsiella pneumoniae. J Biol Chem **285:**19668–19687. http://dx.doi.org/10.1074/jbc.M110.122598.
17. **McNulty C, Thompson J, Barrett B, Lord L, Andersen C, Roberts IS.** 2006. The cell surface expression of group 2 capsular polysaccharides in Escherichia coli: the role of KpsD, RhsA and a multi-protein complex at the pole of the cell. Mol Microbiol **59:**907–922. http://dx.doi.org/10.1111/j.1365-2958.2005.05010.x.
18. **Formstone A, Carballido-Lopez R, Noirot P, Errington J, Scheffers DJ.** 2008. Localization and interactions of teichoic acid synthetic enzymes in Bacillus subtilis. J Bacteriol **190:**1812–1821. http://dx.doi.org/10.1128/JB.01394-07.
19. **Steenbergen SM, Vimr ER.** 2008. Biosynthesis of the Escherichia coli K1 group 2 polysialic acid capsule occurs within a protected cytoplasmic compartment. Mol Microbiol **68:**1252–1267. http://dx.doi.org/10.1111/j.1365-2958.2008.06231.x.
20. **Sambrook J, Fritsch EF, Maniatis T.** 1989. Molecular cloning: a laboratory manual, 2nd ed. Cold Spring Harbor Laboratory Press, Cold Spring Harbor, NY.
21. **Karimova G, Pidoux J, Ullmann A, Ladant D.** 1998. A bacterial two-hybrid system based on a reconstituted signal transduction pathway. Proc Natl Acad Sci U S A **95:**5752–5756. http://dx.doi.org/10.1073/pnas.95.10.5752.
22. **Miller JH.** 1972. Experiments in molecular genetics. Cold Spring Harbor Laboratory, Cold Spring Harbor, NY.
23. **Briones G, Inon de Iannino N, Steinberg M, Ugalde RA.** 1997. Periplasmic cyclic 1,2-beta-glucan in Brucella spp. is not osmoregulated. Microbiology **143:**1115–1124. http://dx.doi.org/10.1099/00221287-143-4-1115.
24. **Lowry OH, Rosebrough NJ, Farr AL, Randall RJ.** 1951. Protein measurement with the Folin phenol reagent. J Biol Chem **193:**265–275.
25. **Hallez R, Mignolet J, Van Mullem V, Wery M, Vandenhaute J, Letesson JJ, Jacobs-Wagner C, De Bolle X.** 2007. The asymmetric distribution of the essential histidine kinase PdhS indicates a differentiation event in Brucella abortus. EMBO J **26:**1444–1455. http://dx.doi.org/10.1038/sj.emboj.7601577.
26. **Ruiz-Ranwez V, Posadas DM, Van der Henst C, Estein SM, Arocena GM, Abdian PL, Martin FA, Sieira R, De Bolle X, Zorreguieta A.** 2013. BtaE, an adhesin that belongs to the trimeric autotransporter family, is required for full virulence and defines a specific adhesive pole of Brucella suis. Infect Immun **81:**996–1007. http://dx.doi.org/10.1128/IAI.01241-12.
27. **Lupas A, Van Dyke M, Stock J.** 1991. Predicting coiled coils from protein sequences. Science **252:**1162–1164. http://dx.doi.org/10.1126/science.252.5009.1162.
28. **Karimova G, Dautin N, Ladant D.** 2005. Interaction network among Escherichia coli membrane proteins involved in cell division as revealed by bacterial two-hybrid analysis. J Bacteriol **187:**2233–2243. http://dx.doi.org/10.1128/JB.187.7.2233-2243.2005.
29. **Sugiura N, Baba Y, Kawaguchi Y, Iwatani T, Suzuki K, Kusakabe T, Yamagishi K, Kimata K, Kakuta Y, Watanabe H.** 2010. Glucuronyltransferase activity of KfiC from Escherichia coli strain K5 requires association of KfiA: KfiC and KfiA are essential enzymes for production of K5 polysaccharide, N-acetylheparosan. J Biol Chem **285:**1597–1606. http://dx.doi.org/10.1074/jbc.M109.023002.
30. **Van der Henst C, de Barsy M, Zorreguieta A, Letesson JJ, De Bolle X.** 2013. The Brucella pathogens are polarized bacteria. Microbes Infect **15:**998–1004. http://dx.doi.org/10.1016/j.micinf.2013.10.008.
31. **Deghelt M, Mullier C, Sternon JF, Francis N, Laloux G, Dotreppe D, Van der Henst C, Jacobs-Wagner C, Letesson JJ, De Bolle X.** 2014. G1-arrested newborn cells are the predominant infectious form of the pathogen Brucella abortus. Nat Commun **5:**4366. http://dx.doi.org/10.1038/ncomms5366.
32. **Van der Henst C, Beaufay F, Mignolet J, Didembourg C, Colinet J, Hallet B, Letesson JJ, De Bolle X.** 2012. The histidine kinase PdhS controls cell cycle progression of the pathogenic alphaproteobacterium Brucella abortus. J Bacteriol **194:**5305–5314. http://dx.doi.org/10.1128/JB.00699-12.
33. **Posadas DM, Ruiz-Ranwez V, Bonomi HR, Martin FA, Zorreguieta A.** 2012. BmaC, a novel autotransporter of Brucella suis, is involved in bacterial adhesion to host cells. Cell Microbiol **14:**965–982. http://dx.doi.org/10.1111/j.1462-5822.2012.01771.x.